

OPEN

Transmembrane signaling on a protocell: Creation of receptor-enzyme chimeras for immunodetection of specific antibodies and antigens

Jiulong Su¹, Tetsuya Kitaguchi², Yuki Ohmuro-Matsuyama², Theresa Seah³, Farid J. Ghadessy⁴, Shawn Hoon³ & Hiroshi Ueda^{2*}

It is known that digital counting of fluorescent signals generated in many small compartments can significantly improve the detection sensitivity of the enzyme-linked immunosorbent assay (ELISA). However, the reported digital ELISA systems need extensive washing steps to remove background signal, which hampers their performance. To tackle this problem, we developed a vesicle (Protocell) array wherein binding of an external protein analyte is coupled to signal amplification and intra-vesicular fluorescence readout. We chose β -glucuronidase (GUS) as a reporter enzyme as its function requires assembly of four subunits through dimerization of a pair of dimers that can be inhibited by a set of interface mutations. Using a thermostabilized GUS mutant IV-5, we screened out an interface mutant (M516K, F517W) to create IV5_m - a mutant with high thermostability and activity conditional on induced dimerization. After tethering a short N-terminal tag and transmembrane (TM) sequences, the fusion protein was expressed by cell-free protein synthesis inside protocells. When a corresponding tag-specific antibody was applied outside of the protocells, a clear increase in GUS activity was observed inside vesicles by adding fluorescent substrate, probably due to spontaneous integration of the tagged TM protein into the vesicles and dimerization by the antibody bound to the displayed tag. Furthermore, using flow cytometry, quantitative digital read out was obtained by counting fluorescent protocells exposed to varying concentrations of external antibodies that included Trastuzumab. Additionally, through use of an anti-caffeine V_{HH}-SpyCatcher fusion protein, caffeine could be detected using SpyTag-fused TM-IV5_m protein expressed in protocells, suggesting utility of this platform for detection of diverse antigen types.

The immunoassay can detect various targets by antigen-antibody interaction with high sensitivity and specificity. Compared with traditional analytical methods such as spectroscopy and chromatography, the immunoassay is faster and more convenient¹. Many types of immunoassays such as sandwich enzyme-linked immunosorbent assay (ELISA) have been widely used². Recently, ELISA systems performed on microchambers to give digital counting of binding signals were reported to significantly increase the detection sensitivity^{3,4}. However, like the traditional ELISA method, extensive washing steps are also needed for this digital ELISA system to remove background signal, which hampers its performance. Meanwhile, protocell arrays have been deployed for sensitive DNA analysis that provides a digitized signal^{5,6}. Creation of a protocell array that amplifies the binding signal of

¹Graduate School of Life Science and Technology, Tokyo Institute of Technology, 4259-R1-18 Nagatsuta-cho, Midori-ku, Yokohama, Kanagawa, 226-8503, Japan. ²Laboratory for Chemistry and Life Science, Institute of Innovative Research, Tokyo Institute of Technology, 4259-R1-18 Nagatsuta-cho, Midori-ku, Yokohama, Kanagawa, 226-8503, Japan. ³Molecular Engineering Laboratory, Biomedical Sciences Institutes, Agency for Science Technology and Research (A*STAR), 61 Biopolis Drive, Singapore, 138673, Singapore. ⁴p53 Laboratory, Agency for Science Technology and Research (A*STAR), 8A Biomedical Grove, Singapore, 138673, Singapore. *email: ueda@res.titech.ac.jp

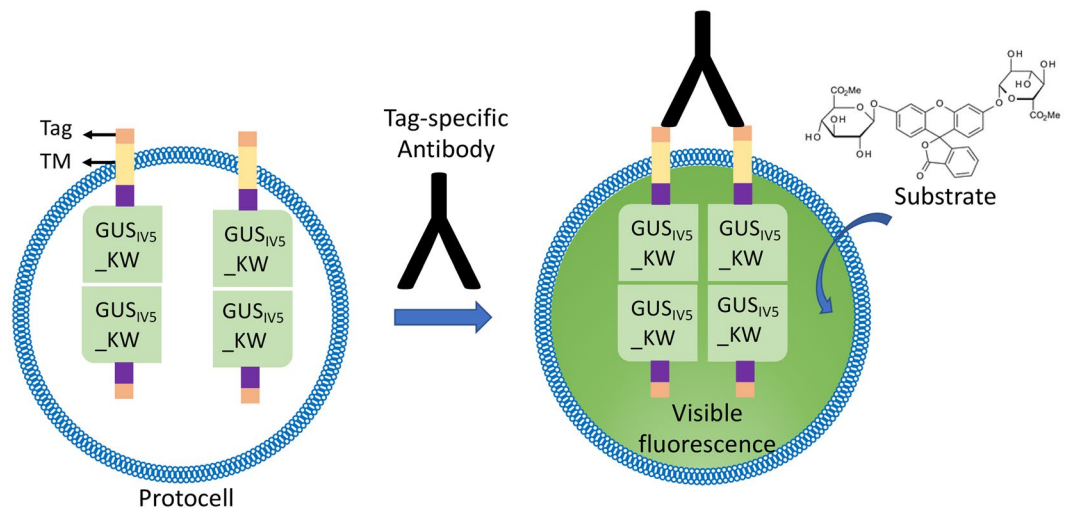


Figure 1. Scheme depicting detection of tag-specific antibodies using engineered protocells. External binding of a bivalent target such as antibody results in intra-vesicular enzyme dimerization and signal generation. To facilitate display of TM-fused subunit, non TM-fused subunit was co-expressed.

external protein as a fluorescent signal of individual protocell will be a powerful clue to tackle this drawback of digital ELISA.

A variety of model membranes have been developed to construct bilayer vesicles in different sizes. Among them giant unilamellar vesicles (GUVs), referred to here as protocells, have a diameter larger than 1 μm and are ideal vesicles for an array system due to their similar size to cells and absence of organelles⁷. Protocells formed by inverted emulsion system and incorporated with the *in vitro* protein translation system have proved to be efficient in synthesized functional proteins such as green fluorescence protein (GFP)⁸ and transmembrane proteins^{9,10}.

In natural cells, extracellular ligand binding signal is usually transduced by transmembrane receptors, and in many cases, dimerization of the receptor intracellular domain triggers activation of enzymes including kinases and subsequent signaling cascade. However, reconstruction of natural signaling cascades to get reliable signal in individual protocells is considered difficult. To mimic such natural signaling, here we used mutant beta-glucuronidase (GUS) as an alternative signal generator. GUS is a self-assembling tetrameric enzyme that catalyzes breakdown of complex carbohydrates. The tetramer state is necessary for the activity of GUS¹¹ and can be prevented by a set of interface mutations¹². Previously, a thermostabilized mutant of GUS (GUS_{IV5})¹³ was used to screen out a set of interface mutations (M516K, F517W) to give GUS_{IV5}-KW which shows high activity when tetramerized and low background at the inactive dimer state¹⁴. In order to transduce an external ligand binding event to generate intra-protocellular signal, the transmembrane (TM) sequence from human epidermal growth factor receptor (EGFR)¹⁵ with epitope tags on its N-terminal was tethered to GUS_{IV5}-KW to make fusion proteins with membrane spanning capability capable of generating a ligand-dependent fluorescence signal (Fig. 1).

As the external targets, we first chose several common used anti-tag antibodies. The bivalent nature of these IgG antibodies is expected to dimerize the two membrane-exposed tag sequences, which will drive the association of tethered GUS_{IV5}-KW domains inside protocells. Secondly, in view of practical application in therapeutic drug monitoring (TDM), we tried to detect Trastuzumab, a human anti-Her2 antibody using a mimotope sequence¹⁶ instead of epitope. Finally, to expand the scope of this protocell system, we employed SpyCatcher-SpyTag technology¹⁷ to prepare a nanobody (V_{HH})¹⁷-fused SpyCatcher protein, and applied it to SpyTag-displaying protocells for detection of the membrane impermeable small antigen caffeine.

Results

Display of His-tag on the surface of protocell membrane. We first chose His-tag (HHHHHH) as a model epitope because of its short length and moderate hydrophobicity. To make protocells that display His-tag on their surface and transmit antibody-mediated dimerization signal into their interior, His₆-TM-GUS_{IV5}-KW protein was synthesized by *in vitro* transcription/translation using a cell-free translation system with pure components (PUREfrex[®] 1.0) in protocells prepared by inverted emulsion method as described in the experimental section. We expected that the short tag sequence immediately after the N-terminal methionine of synthesized fusion protein can spontaneously traverse the lipid bilayer, and be displayed on the outer membrane surface with the aid of EGFR TM. To confirm the display of His₆ tag, we incubated the recovered protocells serially with biotin-conjugated anti-His₆ antibody and streptavidin-phycoerythrin (PE) (Supplementary Fig. S1a). After washing the excess dye, protocells labeled with PE were clearly observed under the fluorescence microscope. On the contrary, no fluorescence was observed when no antibody was used (Supplementary Fig. S1b). Hence, the N-terminal His₆-tag was confirmed to be displayed on the surface of protocell, revealing the spontaneous integration of TM domain of the fusion protein into protocell membrane.

Qualitative detection of tag-specific antibodies using protocells. To attain transmembrane signaling by the dimerization of extracellular tag sequences, His₆-TM-GUS_{IV5}-KW protein was synthesized alone

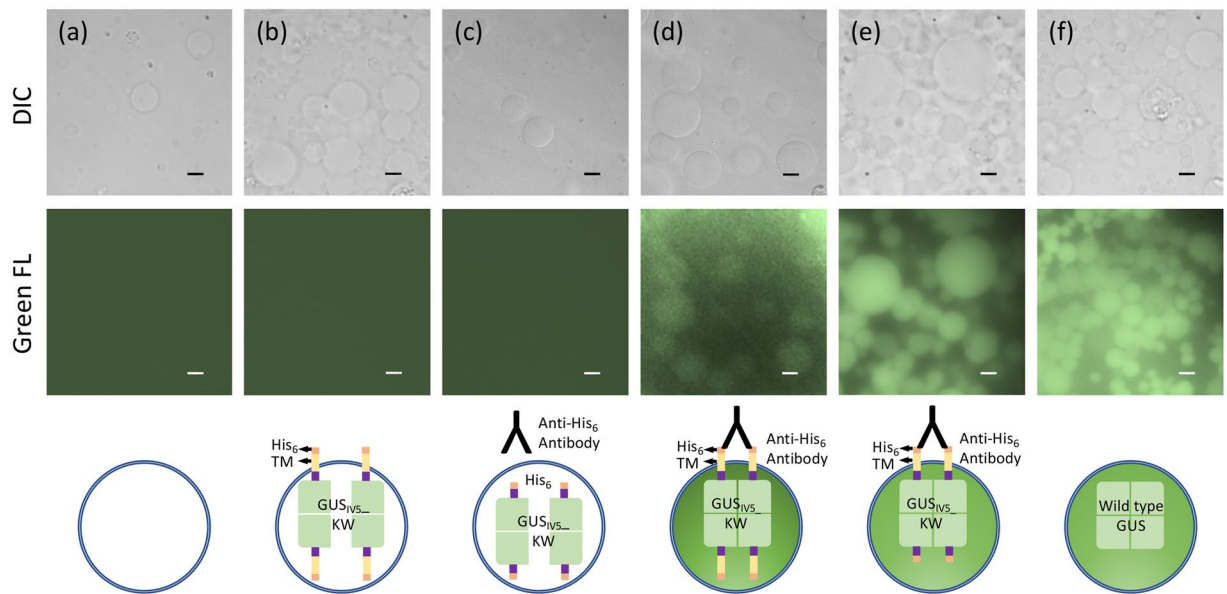


Figure 2. Differential interference contrast (DIC) (upper) and green fluorescence (lower) images of the protocells displaying His₆-tag after substrate treatment. (a) Protocells without protein synthesized, (b) Protocells His₆-TM-GUS_{IV5}-KW protein synthesized, (c) Protocells with His₆-GUS_{IV5}-KW protein synthesized and treated with 0.1 μM anti-His₆ antibody, (d) Protocells with His₆-TM-GUS_{IV5}-KW protein synthesized and treated with 0.1 μM anti-His₆ antibody, (e) Protocells with His₆-TM-GUS_{IV5}-KW and His₆-GUS_{IV5}-KW proteins synthesized together and treated with 0.1 μM anti-His₆ antibody, (f) Protocells with wild type GUS synthesized. Scale Bars: 10 μm.

or co-synthesized with His₆-GUS_{IV5}-KW protein without TM in an equimolar amount by controlling the template concentration used for PUREflex reaction to form GUS_{IV5}-KW dimers inside protocells (Fig. 1). After isolation of protocells with expressed fusion proteins and adding membrane-permeable fluorogenic substrate fluorescein di-β-D-glucuronide (FDGlcU) dimethyl ester, fluorescein generated by the enzyme reaction gave the protocell visible green fluorescence under microscopy (Fig. 2). Since the cleavage of substrate by GUS liberates more hydrophilic carboxyfluorescein, it was considered to remain within the protocells. As negative and positive controls, protocells with no synthesized protein (Fig. 2a) and with the wild-type GUS synthesized (Fig. 2f) were taken, respectively. Remarkably, after adding anti-His₆ antibody to the protocells expressing His₆-TM-GUS_{IV5}-KW protein and incubation for 30 min, a clear antibody-dependent fluorescence of the protocells was observed, probably reflecting the activation of GUS activity due to the dimerization of dimeric fusion proteins induced by antibody binding (Fig. 2b,d). Interestingly, the protocells co-expressing His₆-TM-GUS_{IV5}-KW and His₆-GUS_{IV5}-KW (Fig. 2e) showed even stronger fluorescence than the protocells expressing His₆-TM-GUS_{IV5}-KW alone, probably due to membrane-free His₆-GUS_{IV5}-KW protein in the protocell that could preferentially form a dimer with His₆-TM-GUS_{IV5}-KW bound on the membrane without unfavorable entropic loss, and could give more stable active tetramers after antibody binding. As another negative control, the protocells expressing TM-free His₆-GUS_{IV5}-KW protein alone did not show detectable fluorescence even in the presence of anti-His₆ antibody (Fig. 2b). This clearly shows the necessity of a TM sequence for the display of His tag on the protocell. Considering the higher display efficiency of TM-encoding fusion proteins, in the following experiments, His₆-GUS_{IV5}-KW without TM sequence was always co-synthesized with transmembrane fusion proteins to obtain better fluorescence signal.

To show the generality of anti-tag antibody detection by the tag-displaying protocells, HA (YPYDVPDYA) and Myc (EQKLISEEDL) tags were displayed similarly on the protocell surface by constructing and synthesizing HA-TM-GUS_{IV5}-KW and Myc-TM-GUS_{IV5}-KW proteins together with His₆-GUS_{IV5}-KW protein using the same method. After applying anti-HA antibody and anti-Myc antibody in the extravesicular solution, respectively, fluorescence caused by the antibody-induced enzyme activity was clearly observed under fluorescence microscopy (Fig. 3a–d). The result revealed the successful display of these short tags and the conversion of extravesicular antibody binding signal to intra-protocellular fluorescence signal.

Quantitative detection of anti-His₆ antibody using protocells. To quantify the fluorescence signal and measure the extravesicular antibody dose-response, protocells labeled with rhodamine-DHPE which expressed His₆-TM-GUS_{IV5}-KW and His₆-GUS_{IV5}-KW proteins were incubated with anti-His₆ antibody in gradient concentrations for 30 min at room temperature, and analyzed by flow cytometry after incubation with the substrate for 30 min (Fig. 4a). The green fluorescence showing the GUS activity and the red fluorescence showing the size of individual protocells were then plotted to discriminate GUS-positive protocells (Fig. 4b–e). A region was set so that when no antibody was added, the population of protocells showing higher enzyme activity than background was zero, and the same region was used for counting fluorescein-positive cells, throughout a series of

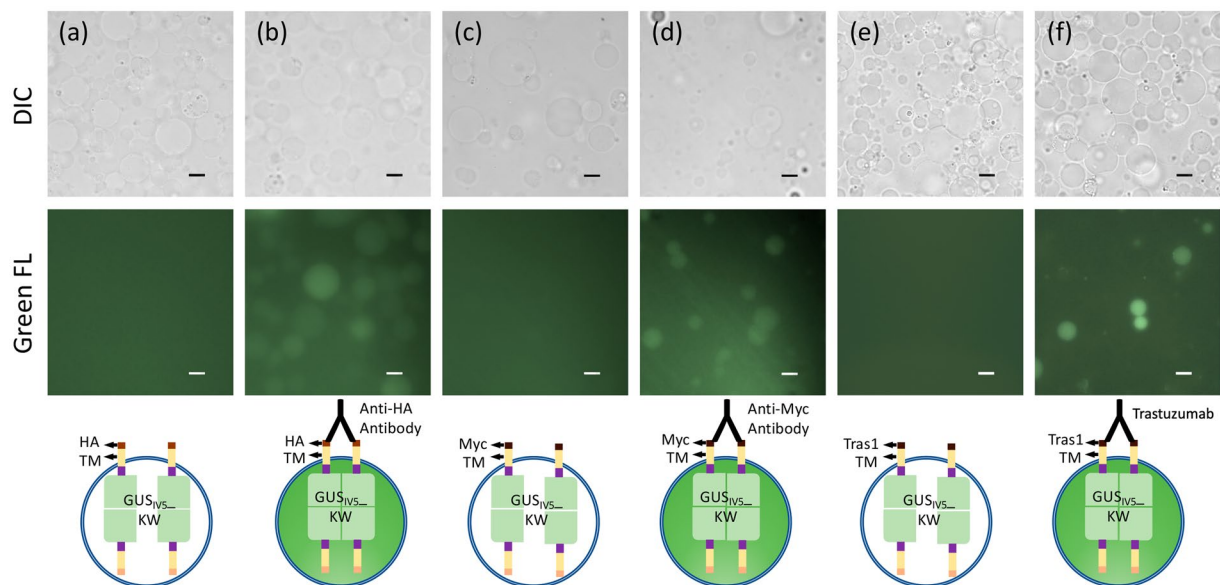


Figure 3. DIC (upper) and green fluorescence (lower) images of the protocells displaying HA-tag, myc-tag, and anti-Her2 mimotope. **(a,b)** Protocells with HA-TM-GUS_{IV5}-KW and His₆-GUS_{IV5}-KW proteins synthesized, and treated with 0.1 μM anti-HA antibody in **(b)**, **(c,d)** Protocells with Myc-TM-GUS_{IV5}-KW and His₆-GUS_{IV5}-KW proteins synthesized, and treated with 0.1 μM anti-myc antibody in **(d)**. **(e,f)** Protocells with Tras1 mimotope-TM-GUS_{IV5}-KW and His₆-GUS_{IV5}-KW proteins synthesized, and treated with 1 μM Trastuzumab in **(f)**. Scale Bars: 10 μm

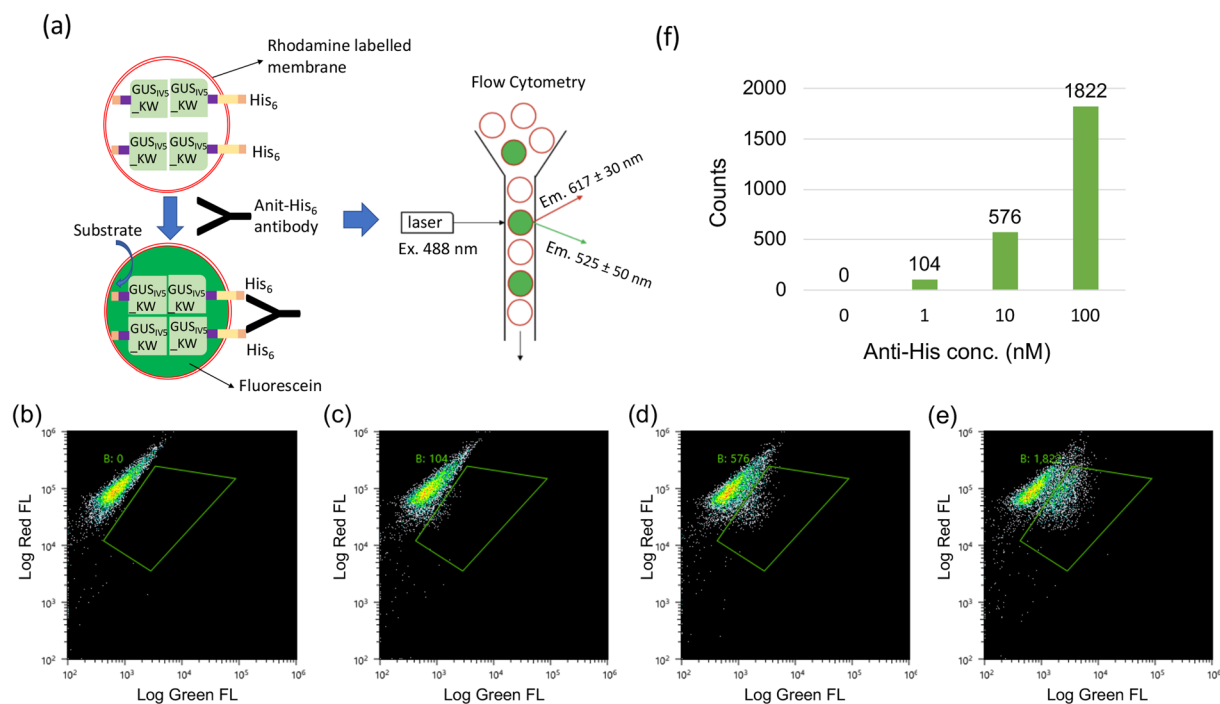


Figure 4. Digital detection of anti-His antibody. **(a)** Scheme of flow cytometric analysis for protocells. **(b-e)** Flow cytometric analysis for protocells displaying His₆-tag responding to anti-His₆ antibody in gradient concentrations of 0 nM **(b)**, 1 nM **(c)**, 10 nM **(d)** and 100 nM **(e)**. **(f)** Event counts for the GreenFL-positive protocells in the selected region at the respective anti-His₆ antibody concentration.

measurements. When the antibody concentration was increased, the counts of protocells showing higher enzyme activity increased correspondingly. By obtaining the event counts of the fraction with antibody induced enzyme activity, a digital signal corresponding to antibody concentration was obtained (Fig. 4f).

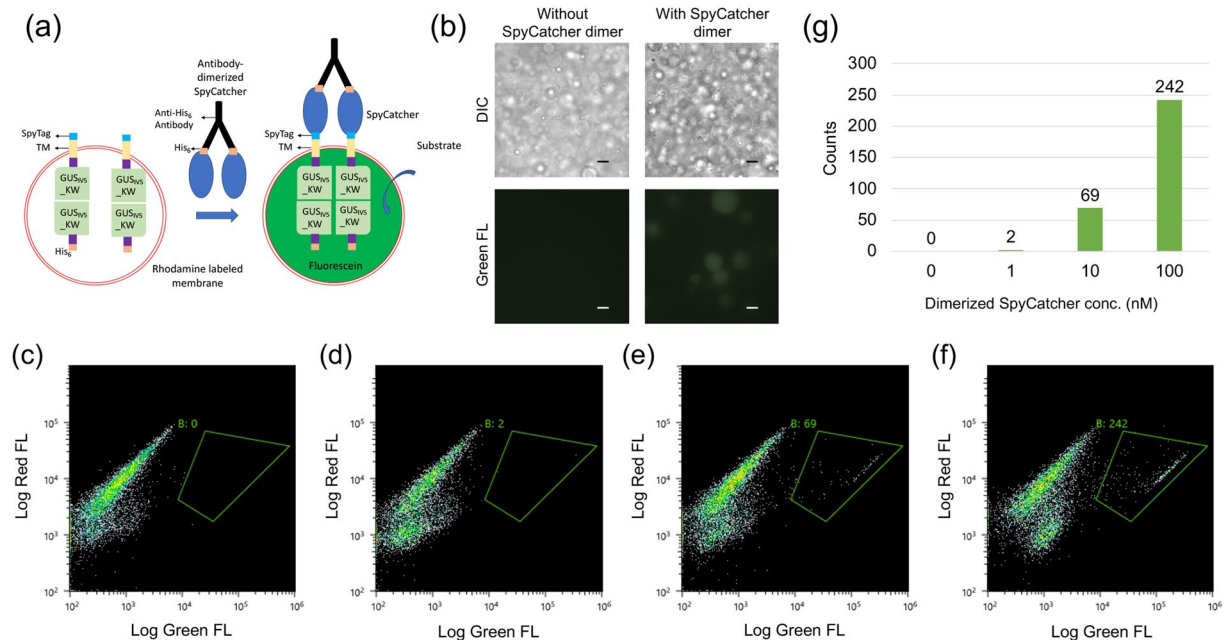


Figure 5. Detection of SpyCatcher dimers. **(a)** Scheme for protocells displaying SpyTag activated by antibody-dimerized SpyCatcher binding. **(b)** DIC (upper) and fluorescence (lower) microscopy of stabilized protocells without rhodamine-DHPC displaying SpyTag, with and without addition of 0.1 μM SpyCatcher dimer after 3 h incubation with substrate. Scale Bars: 10 μm. **(c–f)** Flow cytometric analysis for protocells displaying SpyTag responding to SpyCatcher dimer at 0 nM **(c)**, 1 nM **(d)**, 10 nM **(e)**, and 100 nM **(f)**. **(g)** Event counts for the positive protocells at the respective SpyCatcher dimer concentration.

Quantitative detection of trastuzumab using protocells. To investigate the possible use of this system in TDM, a Trastuzumab mimotope sequence (TRAS-1: QLGPYELWELSH)¹⁶ was cloned into the N-terminal of TM-GUS_{IV5}-KW sequence, and quantitative detection of Trastuzumab was tested similarly to anti-His tag antibody. To increase the fluorescent signal, we tried to increase protocell membrane stability by altering membrane composition through addition of PEG2000PE and more cholesterol¹⁸, and extended the incubation time to 3 h. After applying Trastuzumab in the extravesicular solution, fluorescence caused by the antibody-induced enzyme activity was clearly observed under fluorescence microscopy (Fig. 3e–f). Also, when the protocells incubated with varying concentrations of Trastuzumab were analyzed by FCM, similar results to anti-His antibody detection were obtained (Supplementary Fig. S2). It is worth noting that compared with the original bioluminescence resonance energy transfer-based sensor (TRAS-LUMABS-1)¹⁶, a lower concentration of 10 nM Trastuzumab could be detected.

Detection of dimerized SpyCatcher protein by protocells displaying SpyTag. SpyTag/SpyCatcher is a powerful covalent isopeptide conjugation system for bioconjugation and engineering protein architectures^{17,19}. To test the possibility of applying SpyTag/SpyCatcher system as a connector between the protocell biosensor and an extracellular binding domain such as an antibody fragment, an expression vector for SpyTag-TM-GUS_{IV5}-KW was constructed. This protein and His₆-GUS_{IV5}-KW without TM were next synthesized inside protocells with improved membrane composition as in the Trastuzumab detection. To investigate the functional ligation of SpyTag/SpyCatcher, His₆-SpyCatcher protein was expressed in *E. coli* (Supplementary Fig. S3) and dimerized by anti-His₆ antibody (Fig. 5a). After SpyCatcher dimers in different concentrations were incubated with protocell carrying SpyTag-TM-GUS_{IV5}-KW protein for 3 h at room temperature, microscopic observation and flow cytometric analysis were performed to measure the size and enzyme activity of protocells as previously described. As a result, SpyTag-displaying protocells incubated with SpyCatcher dimers were clearly observed under fluorescence microscopy (Fig. 5b) and the counts of protocells showing enzyme activity caused by GUS tetramerization increased correspondingly to the concentration of SpyCatcher dimers (Fig. 5c–f). From the protocell counts of the region with antibody induced enzyme activity, a quantified signal corresponding to antibody concentration can be obtained (Fig. 5g). The lower counts compared to His₆-tag displaying protocells might indicate the lower display efficiency of SpyTag and/or lower efficiency of dimerization compared with direct His₆-tag crosslinking, which might also result in difficulties observing fluorescent protocells using the original membrane composition by microscopy (Supplementary Fig. S4). However, we could still perform FCM analysis of those original protocells with lower fluorescent intensities in 30 min (Supplementary Fig. S5).

Detection of caffeine using anti-caffeine V_{HH}-SpyCatcher protein and protocells displaying SpyTag. Next, we employed a nanobody (V_{HH})-SpyCatcher fusion protein instead of His₆-SpyCatcher protein to drive protocell signal transduction. Interestingly, an anti-caffeine V_{HH} was reported to show hapten-induced

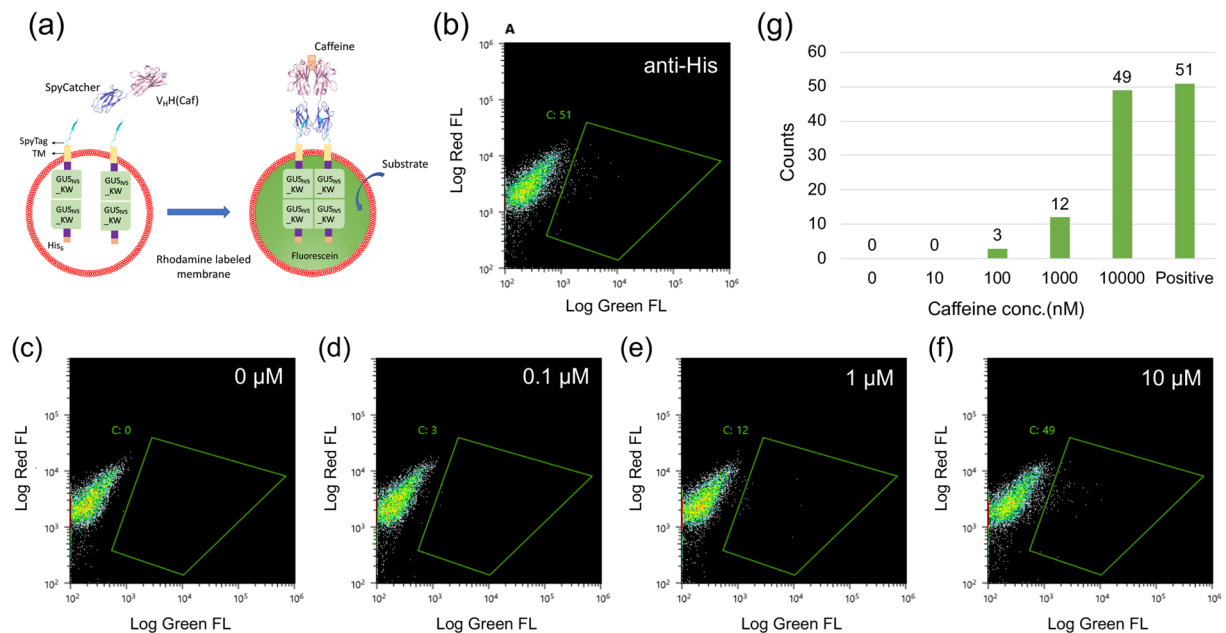


Figure 6. Detection of Caffeine. (a) Scheme for protocells displaying SpyTag activated by antigen-dimerized V_{HH}-SpyCatcher. (b) Modified protocells displaying SpyTag with and without 0.1 μM SpyCatcher dimer after 3 h incubation with substrate. (b–f) Flow cytometric analysis for protocells displaying SpyTag responding to V_{HH}-SpyCatcher dimer in the presence of 0.1 μM anti-His antibody (b) or 0 nM (c), 0.1 μM (d), 1 μM (e) and 10 μM (f) of caffeine. (g) Event counts for the positive protocells at the respective SpyCatcher dimer concentration.

dimerization¹⁴. Based on this idea, an expression vector for adaptor protein consisting of anti-caffeine V_{HH} fused with SpyCatcher was made, and the protein expressed in *E. coli* SHuffle T7 express lysY and purified to homogeneity (Supplementary Fig. S6).

V_{HH}-SpyCatcher in the presence of different concentrations of caffeine or 0.1 μM anti-His antibody as a positive control was incubated with protocell carrying SpyTag-TM-GUS_{IVS}-KW protein for 3 h at room temperature. Flow cytometry was then used to measure the size and enzyme activity of protocells as before (Fig. 6). The number of protocells showing enzyme activity caused by GUS tetramerization increased upon addition of anti-His antibody (Fig. 6b,c) and further corresponded to the caffeine concentration (Fig. 6c–f). From the counts of protocells in the region with increased Green FL, a quantified signal corresponding to caffeine concentration was obtained (Fig. 6g). Caffeine is present in many widely consumed beverages, and it can be toxic to adults at intake levels exceeding 500 mg per day²⁰. Considering that the caffeine concentration of tea is approximately 140 μM and that in coffee is approximately 5 mM²¹, this system will be able to detect caffeine in common foods and beverages.

Discussion

In this study, a protocell-based biosensor system was constructed and successfully used for the detection of tag-specific antibodies and a small antigen that drives dimerization of its binding nanobody. Compared with other solution-based biosensor systems, the protocell increases sensitivity by decreasing the background signal and providing signals in an “on/off” manner. The simpler system than digital ELISA improved assay handling; the protocell biosensor does not need any separation steps before measurement and permits assay in a one-step reaction. This gives the protocell system a great potential to serve as an efficient detection method. Furthermore, the successful detection of Trastuzumab indicates the system’s potential application in TDM. Compared with other enzyme-based biosensors, the proposed system has an additional merit that it is insensitive to possible intrinsic enzyme (GUS) activity in samples such as body fluid. Additionally, the positive responses to externally dimerized SpyCatcher by SpyTag displaying protocells will make it possible to detect various targets by fusing SpyCatcher with not only nanobodies but with many other binding domains, such as single chain antibody fragments.

To understand the detectability of a single activated enzyme tetramer in one protocell, which is considered necessary to obtain single molecule-derived digital signal³, the amount of final product of the enzyme reaction was calculated. Based on the turnover number K_{cat} of GUS_{IVS}-KW protein for the fluorescent substrate measured as 1.18 s^{-1} (Supplementary Fig. S7), it was calculated that in a protocell with 2 μm diameter containing one molecule of fully activated GUS_{IVS}-KW can give 45 nM fluorescein in this protocell after 1 h of reaction. If a more stable protocell is used to extend the reaction time to 3 h, 135 nM fluorescein will be obtained. When we prepared a set of protocells with varied concentrations of fluorescein inside and measured their signal by flow cytometry, the protocells with 100 nM fluorescein inside were easily detectable by this method (Supplementary Fig. S8). This means that the protocell biosensor system will be able to provide digital read outs by controlling the size and the amount of proteins synthesized.

By providing low background and a digitalized signal, sensitivity of this protocell biosensor system for use in immunodetection has been greatly increased. Considering the potential in detecting multiple targets and protein interactions, the developed protocell biosensor system will be very useful in immunological studies and medical diagnostic settings.

Experimental

Materials. 1-Palmitoyl-2-oleoyl-sn-glycero-3-phosphocholine (POPC) was purchased from NOF corporation (Tokyo, Japan), cholesterol was from Nacalai Tesque (Kyoto, Japan), and 1,2-distearoyl-sn-glycero-3-phosphoethanolamine-N-[methoxy (polyethylene glycol)-2000] (PEG2000PE) was purchased from Avanti Polar Lipids (Alabaster, AL, USA). Biotin-conjugated anti-PentaHis antibody was purchased from Qiagen Japan (Tokyo, Japan). Streptavidin-PE was purchased from Miltenyi Biotec (Bergisch Gladbach, Germany). Rhodamine B 1, 2-dihexadecanoyl-sn-glycero-3-phosphoethanolamine, triethylammonium salt (rhodamine-DHPE) was purchased from Setareh Biotech (Eugene, OR, USA). PUREfret 1.0 system was purchased from GeneFrontier (Chiba, Japan). The expression vector for His-Avi-tagged SpyCatcher002 (pDEST14-Avitag-SpyCatcher002) was obtained from Addgene (Watertown, MA, USA). The DNA encoding SpyTag002 was synthesized by Eurofin Genomics (Tokyo, Japan). *E. coli* SHuffle T7 Express lysY for protein expression and the restriction enzymes were obtained from NEB Japan (Tokyo, Japan). Monoclonal anti-His (28–75), anti-HA, and anti myc antibodies was from Fujifilm Wako. Other chemicals were purchased from Fujifilm Wako Chemicals (Tokyo, Japan).

The following oligonucleotides were synthesized by Eurofin Genomics, and used:

His_NdeI_Back: 5'-AAGGAGATATACATATGCACCATCATCATCATCAT-3'
 His_HindIII_For: 5'-ACCGCCACCAAGCTTATGATGATGATGATGGTGCA-3'
 TM_His_For: 5'-CATCCCAGTGGCGATATGATGATGATGATGGTGCA-3'
 HA_NdeI_Back: 5'-AAGGAGATATACATATGTATCCGTATGATGTGCCG-3'
 TM_HA_For: 5'-CATCCCAGTGGCGATCGCATAATCCGGCACATCA-3'
 Myc_NdeI_Back: 5'-AAGGAGATATACATATGGAACAGAACTGATTAGC-3'
 TM_Myc_For: 5'-CATCCCAGTGGCGATCAGATCTTCTTCGCTAATCA-3'
 TM_Tras1_For: 5'-CATCCCAGTGGCGATATGCGACAATCCCAATTCGTAAGG-3'
 NdeTras1_Back: 5'-AAGGAGATATACATATGCAGTTAGGCCCTTACGAATTGTGGG-3'
 Spy_NdeI_Back: 5'-AAGGAGATATACATATGGTGCCTACTATCGTGATG-3'
 TM_Spy_For: 5'-CATCCCAGTGGCGATCTGTAAACGCTTGTAGGC-3'
 TM_Back: 5'-ATCGCCACTGGGATGG-3'
 TM_HindIII_For: 5'-CACCGCCACCAAGCTTCATGAAGAGGCCGATCCC-3'
 VHH-SpyCatcher_Infus_Back: 5'-GGTAGCGCGCCGCTATGGTAACCACCTTATC-3'
 VHH-SpyCatcher_Infus_For: 5'-GTGGTGGTCTCGAGTTAGCTACCACTGGATCC-3'

Construction of plasmids. His₆-tag, HA-tag, Myc-tag and SpyTag DNAs were amplified as primer dimers by using the primer pairs His_NdeI_Back/TM_His_For, HA_NdeI_Back/TM_HA_For, Myc_NdeI_Back/TM_Myc_For, NdeTras1_Back/TM_Tras1_For and Spy_NdeI_Back/TM_Spy_For using a thermal cycler. The sequence encoding the transmembrane domain (TM) of human EGFR was amplified by PCR using TM_Back and TM_HindIII_For primers and pCO12-EGFR (Riken Bioresource Center, Tsukuba, Japan) as a template. DNAs of tags were fused to TM DNA by overlap extension PCR to give His₆-TM, HA-TM, Myc-TM, Tras1-TM and SpyTag-TM DNAs. In short, His₆-TM, HA-TM, Myc-TM, Trans1-TM and Spy-TM sequences were inserted into GUS_{IV5}-KW vector linearized by *NdeI* and *HindIII*, using an In-Fusion™ HD cloning kit (Takara-Bio, Shiga, Japan) to construct His₆-TM-GUS_{IV5}-KW, HA-TM-GUS_{IV5}-KW, Myc-TM-GUS_{IV5}-KW, Trans1-GUS_{IV5}-KW and SpyTag-TM-GUS_{IV5}-KW vectors. His₆-tag DNA with *NdeI* and *HindIII* restriction enzyme sites was amplified by PCR using His_NdeI_Back and His_HindIII_For primers and inserted into linearized GUS_{IV5}-KW vector with same restriction enzyme sites to construct His₆-GUS_{IV5}-KW vector. The expression vector for V_HH(Caf)-SpyCatcher protein was constructed by replacing GUS_{IV5}-KW gene in pET32-V_HH(Caf)-GUS_{IV5}-KW¹⁴ with SpyCatcher002 gene amplified from pDEST14-Avitag-SpyCatcher002 with primers VHH-SpyCatcher_Infus_Back and VHH-SpyCatcher_Infus_For.

Preparation of protocells. The protocells were prepared based on the inverted emulsion methods described by K. Nishimura *et al.*⁸. POPC and cholesterol dissolved in chloroform (100 mg/ml) were mixed in a 9:1 weight ratio in 400 µl paraffin, and water in oil emulsion was made by vortex for 30 s with 20 µl PUREfret 1.0 system reaction mixture including 10 ng/µl template DNA, 1 µl (40 unit) of RNase inhibitor (Nippon Gene, Toyama, Japan) and 330 mM sucrose. After layering the emulsion (400 µl) on 150 µl of outer buffer (100 mM HEPES, 280 mM potassium glutamate, 20 mM Mg(OAc)₂, NTPs (3.75 mM ATP, 2.5 mM GTP, 1.35 mM CTP, 1.35 mM UTP), amino acids (0.3 mM Tyr, 0.3 mM Cys and 0.375 mM for other 18 amino acids), 15 mM creatine phosphate, 330 mM glucose, 20 µg/ml RNase; pH = 7.6) in a microtube, protocells were formed by centrifuge at 18,000 × g for 30 min at 4 °C. Outer buffer containing protocells was collected by piercing the bottom of the tube using a syringe with 18 G × 1 1/2 inch needle.

Detection of enzyme activity. The liposomal suspension was centrifuged at 18,000 × g for 30 min, the supernatant discarded, and 150 µl of the outer buffer was added to resuspend the liposomes. The liposome suspension was incubated for 2 h at 37 °C for protein synthesis. For flow cytometry measurement, 0.1% (w/w) rhodamine-DHPE was included in membrane components. For displaying Tras1 and SpyTag on the protocells, a membrane composition with POPC: cholesterol: PEG2000PE = 5.75: 4: 0.25 in molar ratio¹⁸ was also tested. To the liposome suspension, anti-tag antibody (0.1 µM) was added and incubated at room temperature for 30 min. Afterwards, 0.1 mg/ml fluorescein di-β-D-glucuronide (FDGlcU) dimethyl ester (Marker Gene Technologies,

Eugene, OR, USA) was added as a substrate, and reacted for 30 min (or 3 h for modified protocells composed of POPC, cholesterol and PEG2000PE) at room temperature before microscopic and flow cytometric analyses.

Microscopic observation. Microscopy was performed by an IX 71 inverted microscope (Olympus, Tokyo, Japan). Samples were observed under a 60x objective lens. Fluorescein was excited at 495–500 nm and emission at >505 nm was observed. Phycoerythrin-labeled protocells was excited at 545–580 nm and emission at >600 nm was observed.

Flow cytometric analysis. Flow cytometric analysis was performed using an SH-800 cell sorter (Sony, Tokyo, Japan). Ten thousand events were measured in each flow cytometric analysis. Both rhodamine DHPE and fluorescein were excited at 488 nm. The emission of rhodamine was detected through a 617/30 nm bandpass filter as Red FL and emission of fluorescein was detected through a 525/50 nm bandpass filter as Green FL.

Received: 10 June 2019; Accepted: 13 November 2019;

Published online: 03 December 2019

References

1. Ekins, R. More sensitive immunoassays. *Nature* **284**, 14–15 (1980).
2. Engvall, E. & Perlmann, P. Enzyme-linked immunosorbent assay, Elisa. 3. Quantitation of specific antibodies by enzyme-labeled anti-immunoglobulin in antigen-coated tubes. *J. Immunol.* **109**, 129–135 (1972).
3. Rissin, D. M. *et al.* Single-molecule enzyme-linked immunosorbent assay detects serum proteins at subfemtomolar concentrations. *Nat. Biotechnol.* **28**, 595–599, <https://doi.org/10.1038/nbt.1641> (2010).
4. Kim, S. H. *et al.* Large-scale femtoliter droplet array for digital counting of single biomolecules. *Lab. Chip* **12**, 4986–4991, <https://doi.org/10.1039/c2lc40632b> (2012).
5. Tsugane, M. & Suzuki, H. Reverse transcription polymerase chain reaction in giant unilamellar vesicles. *Sci. Rep.* **8**, 9214, <https://doi.org/10.1038/s41598-018-27547-2> (2018).
6. Joesaar, A. *et al.* DNA-based communication in populations of synthetic protocells. *Nat. Nanotechnol.* **14**, 369–378, <https://doi.org/10.1038/s41565-019-0399-9> (2019).
7. Jorgensen, I. L., Kemmer, G. C. & Pomorski, T. G. Membrane protein reconstitution into giant unilamellar vesicles: a review on current techniques. *Eur. Biophys. J.* **46**, 103–119, <https://doi.org/10.1007/s00249-016-1155-9> (2017).
8. Nishimura, K. *et al.* Cell-free protein synthesis inside giant unilamellar vesicles analyzed by flow cytometry. *Langmuir* **28**, 8426–8432, <https://doi.org/10.1021/la3001703> (2012).
9. Liu, Y. J., Hansen, G. P., Venancio-Marques, A. & Baigl, D. Cell-free preparation of functional and triggerable giant proteoliposomes. *ChemBiochem* **14**, 2243–2247, <https://doi.org/10.1002/cbic.201300501> (2013).
10. Soga, H. *et al.* *In vitro* membrane protein synthesis inside cell-sized vesicles reveals the dependence of membrane protein integration on vesicle volume. *ACS Synth. Biol.* **3**, 372–379, <https://doi.org/10.1021/sb400094c> (2014).
11. Jain, S. *et al.* Structure of human beta-glucuronidase reveals candidate lysosomal targeting and active-site motifs. *Nat. Struct. Biol.* **3**, 375–381 (1996).
12. Geddie, M. L. & Matsumura, I. Antibody-induced oligomerization and activation of an engineered reporter enzyme. *J. Mol. Biol.* **369**, 1052–1059, <https://doi.org/10.1016/j.jmb.2007.03.076> (2007).
13. Flores, H. & Ellington, A. D. Increasing the thermal stability of an oligomeric protein, beta-glucuronidase. *J. Mol. Biol.* **315**, 325–337, <https://doi.org/10.1006/jmbi.2001.5223> (2002).
14. Su, J. *et al.* Creation of stable and strictly regulated enzyme switch for signal-on immunodetection of various small antigens. *J. Biosci. Bioeng.* **128**, 677–682, <https://doi.org/10.1016/j.jbiosc.2019.05.015> (2019).
15. Jura, N. *et al.* Mechanism for activation of the EGF receptor catalytic domain by the juxtamembrane segment. *Cell* **137**, 1293–1307, <https://doi.org/10.1016/j.cell.2009.04.025> (2009).
16. van Rosmalen, M. *et al.* Dual-color bioluminescent sensor proteins for therapeutic drug monitoring of antitumor antibodies. *Anal. Chem.* **90**, 3592–3599, <https://doi.org/10.1021/acs.analchem.8b00041> (2018).
17. Zakeri, B. *et al.* Peptide tag forming a rapid covalent bond to a protein, through engineering a bacterial adhesin. *Proc. Natl. Acad. Sci. USA* **109**, E690–697, <https://doi.org/10.1073/pnas.1115485109> (2012).
18. Berhanu, S., Ueda, T. & Kuruma, Y. Artificial photosynthetic cell producing energy for protein synthesis. *Nat. Commun.* **10**, 1325, <https://doi.org/10.1038/s41467-019-09147-4> (2019).
19. Keeble, A. H. *et al.* Evolving accelerated amidation by SpyTag/SpyCatcher to analyze membrane dynamics. *Angew. Chem. Int. Ed.* **56**, 16521–16525, <https://doi.org/10.1002/anie.201707623> (2017).
20. Heckman, M. A., Weil, J. & Gonzalez de Mejia, E. Caffeine (1, 3, 7-trimethylxanthine) in foods: a comprehensive review on consumption, functionality, safety, and regulatory matters. *J. Food Sci.* **75**, R77–87, <https://doi.org/10.1111/j.1750-3841.2010.01561.x> (2010).
21. Lisko, J. G. *et al.* Caffeine concentrations in coffee, tea, chocolate, and energy drink flavored e-liquids. *Nicotine Tob. Res.* **19**, 484–492, <https://doi.org/10.1093/ntr/ntw192> (2017).

Acknowledgements

We thank Cyrus Beh in Molecular Engineering Laboratory, A*STAR and Yutetsu Kuruma in Earth-Life Science Institute, Tokyo Institute of Technology for helpful discussions. We also thank the Biomaterials Analysis Division, Technical Department, Tokyo Institute of Technology, for DNA sequence analysis. We also thank Riken Bioresource Center, Tsukuba, Japan, for providing pCO12-EGFR plasmid. This work was supported partly by Strategic International Collaborative Research Program (SICORP) and JST-Mirai Program (Grant Number JPMJMI18D9) under Japan Science and Technology Agency, Japan, by JSPS KAKENHI (Grant Numbers JP15H04191, JP18H03851) under the Japan Society for the Promotion of Science, Japan, and Special Research Grant from the Nakatani Foundation, Japan. J.S. was supported by ACEEES Program, Tokyo Institute of Technology.

Author contributions

S.H. and H.U. conceived of the study; J.S. and H.U. designed the experiments; J.S., T.S. and Y.O.M. performed the experiments; J.S., T.K. and H.U. analyzed the results; and J.S. and H.U. wrote the manuscript with input from F.J.G. and S.H.

Competing interests

The authors declare no competing interests.

Additional information

Supplementary information is available for this paper at <https://doi.org/10.1038/s41598-019-54539-7>.

Correspondence and requests for materials should be addressed to H.U.

Reprints and permissions information is available at www.nature.com/reprints.

Publisher's note Springer Nature remains neutral with regard to jurisdictional claims in published maps and institutional affiliations.



Open Access This article is licensed under a Creative Commons Attribution 4.0 International License, which permits use, sharing, adaptation, distribution and reproduction in any medium or format, as long as you give appropriate credit to the original author(s) and the source, provide a link to the Creative Commons license, and indicate if changes were made. The images or other third party material in this article are included in the article's Creative Commons license, unless indicated otherwise in a credit line to the material. If material is not included in the article's Creative Commons license and your intended use is not permitted by statutory regulation or exceeds the permitted use, you will need to obtain permission directly from the copyright holder. To view a copy of this license, visit <http://creativecommons.org/licenses/by/4.0/>.

© The Author(s) 2019